Aerosol Res., 4, 559–576, 2026
https://doi.org/10.5194/ar-4-559-2026
© Author(s) 2026. This work is distributed under
the Creative Commons Attribution 4.0 License.

AEROSOL Research
Open Access



# Assessment of cabin filtration efficiency: contribution to an on-road methodology

**Ambre Delater[1], Sébastien Fable[1], Brice Berthelot[1], Cécile Raventos[1], Jessica Queron[1], Isabelle Coll[2], and Olivier Le Bihan[1]**

[1]INERIS, Parc Technologique ALATA, 60550, Verneuil-en-Halatte, France
[2]Univ Paris Est Creteil and Université Paris Cité, CNRS, LISA, 94010, Créteil, France

**Correspondence:** Jessica Queron (jessica.queron@ineris.fr)

Received: 7 July 2026 – Discussion started: 21 July 2026
Revised: 22 October 2026 – Accepted: 23 October 2026 – Published: 6 November 2026

**Abstract.** The use of cabin filters provides protection for passengers against outdoor pollution caused by particles (aerosols) when travelling by car. Their filtration efficiency is assessed through rigorous laboratory studies in accordance with standards. However, there are few or no comparable studies conducted under real road conditions using reference particle measurements to complement the laboratory results. In this context, our study aims to contribute to the improvement of on-road aerosol measurement by evaluating cabin filters with gravimetric measurements. To this end, a sampling line upstream of the cabin filter in an area located under the windscreen and a sampling point downstream of the cabin filter on the front seat inside the cabin were designed. The sampling efficiency of the line was calculated using a transdisciplinary work involving computational fluid dynamics, wind tunnel measurements, and numerical methods. The results showed that its sampling efficiency for $PM_1$ and $PM_{2.5}$ (i.e. particles with an aerodynamic diameter of less than 1 and 2.5 µm, respectively) is greater than 94 % and 77 %, respectively. Next, on-road tests were carried out in a moving car in the Paris region for two different cabin filters and during tests without a cabin filter. The average filtration efficiency was 54.4 % ($n = 15$), 52.7 % ($n = 14$), and 9.5 % ($n = 4$) for $PM_1$ and 57.6 % ($n = 9$), 56 % ($n = 9$), and 32.0 % ($n = 4$) for $PM_{2.5}$, respectively, for filter A and filter B and without a cabin filter. Lastly, optical counters were simultaneously operated with gravimetric measurements. The results showed that optical counters underestimate the mass concentration of $PM_{2.5}$, highlighting the importance of using a reference method to measure the particles under real road conditions.

## 1 Introduction

Exposure to air pollution results from the accumulation of specific exposure situations that occur in the different environments an individual frequents during the day. In outdoor urban environments, air quality monitoring networks continuously monitor concentrations of regulated pollutants. The measurements made so far have shown a high frequency of exceeding the WHO health protection threshold values, especially for airborne particulate matter (European Environment Agency, 2024b). Literature now acknowledges the central role of repeated exposure to fine particles in the development and exacerbation of chronic respiratory and cardiovascular diseases, which can result in premature death (Gan et al., 2011; Sinharay et al., 2018; Zhang et al., 2024). Such high levels are particularly observed in the vicinity of road traffic as traffic is the third-largest source of $PM_{2.5}$ emissions in Europe, especially its black-carbon fraction (Dons et al., 2013; European Environment Agency, 2024a).

Travelling by car can account for a significant portion of the time spent near vehicle emissions. Using a cabin filter (i.e. filter between outside and the cabin car) in combination with a ventilation system (i.e. HVAC system) can improve indoor air quality and reduce passenger exposure (Heo et al., 2019). However, cabin filters do not all have the same filtration properties, depending on their characteristics (e.g. materials, fibre sizes) (Robert et al., 2023; Xu et al., 2011). Their performance is therefore evaluated on laboratory test benches

(Wang et al., 2024) according to standards (DIN 71460-1, 2006; ISO 12103-1, 2024; ISO/TS 11155-1, 2001).

However, cabin filters are used on the road under conditions that differ from those in a laboratory, e.g. the typology of the environment (rural or urban), the weather conditions (temperature, humidity), the traffic (vehicle speed), the ventilation (on or off), and the composition of particles (Alves et al., 2020; Amato et al., 2011; Xu et al., 2018). These parameters can affect the performance of cabin filters and impact indoor air quality. For example, laboratory tests have shown that the efficiency of a cabin filter can vary depending on the relative humidity and types of particles encountered, such as dust and soot (He et al., 2016). Therefore, there is a need to conduct on-road measurements to complement laboratory studies. However, a reliable measurement methodology must first be developed as there is currently no standard for this.

A reference method for measuring $PM_{10}$ (i.e. particles with an aerodynamic diameter of less than 10 µm) in situ is gravimetry (NF EN 12341, 2023). The gravimetric method can be expensive and unwieldy, making it difficult to install. To determine the mass concentration of particles in the air, the particles are collected on a substrate, such as a filter, which is weighed in a controlled environment (regarding temperature and humidity) using a precision scale. A sufficient mass of particles must be collected for their total weight to exceed the detection limit. This requires the use of bulky pumps in the car to maximise collection. This may explain why only a few studies have implemented gravimetry in a moving car (Greenwald et al., 2014; Kam et al., 2012; Shirmohammadi et al., 2017). To the best of our knowledge, none of these studies evaluated the performance of cabin filters. Conducting this kind of study is particularly challenging as two devices need to be installed: one upstream and one downstream of the cabin filter. The filtration efficiency of the cabin filters on-road was assessed by real-time measurement methods, such as optical particle counters (OPCs) or sensors (Heo et al., 2022; Lee and Zhu, 2014; Liu et al., 2011; Qi et al., 2008; Wei et al., 2020; Yin et al., 2023). Sensors and, more generally, OPCs are easy to set up, take up little space, and provide real-time measurements of several particle sizes simultaneously. Nonetheless, the OPCs cannot measure the absolute mass concentration of particles correctly because (i) they are calibrated with standard particles (e.g. spherical latex particles), (ii) they cannot measure the smallest particles (they have a detection limit), and (iii) they make approximations (measured particles are spherical and have a constant density). This is why it is important to use a reference method to improve on-road aerosol measurements.

Following these observations, the Informal Working Group on Vehicle Interior Air Quality (IWG VIAQ) – set up by the Working Party on Pollution and Energy (GRPE) – proposed the development of harmonised test procedures to address air pollution and interior air-cleaning efficiency under real road conditions (GRPE-70-09-Rev.1, 2015; GRPE-81-09, 2020). In line with the IWG, our study aims to contribute to the development of a methodology for measuring aerosols on the road using a reference method. Specifically, we focused on the filtration of aerosols in the vehicle with cabin filters. We conducted measurements upstream and downstream of a cabin filter. The novelty of this study lies in the design of a sampling line in the scuttle of the car to measure particles upstream of the cabin filter using gravimetric measurements. We also conducted long-duration sampling (up to 6 h) on the road, collecting samples at a rate of 30 L $min^{-1}$ using pumps positioned in the boot. This allowed us to collect sufficient particles to evaluate the cabin filters. Two OPCs were also used in parallel with the gravimetric measurements in order to assess their reliability by comparing the two methods.

This paper presents (i) the evaluation of the sampling efficiency of the upstream line (Sect. 3.2), (ii) the collection of the experimental data (Sect. 3.3), (iii) the comparison between the optical and gravimetric measurements (Sect. 3.4), and (iv) the results of filtration efficiency for two cabin filters (Sect. 3.5).

## 2 Strategy for particle collection

The approach presented here consists of equipping a vehicle for sampling the air on filters for gravimetric measurements upstream and downstream of a cabin filter on the road. The chosen vehicle is a sport utility vehicle. The following paragraphs detail the strategy for collecting particles.

### 2.1 Determination of the cabin filter efficiency

The aerosol filtration efficiency of a media filter ($\eta$) is defined by considering two sampling points, as shown in Eq. (1) (Hinds, 2011):

$$\eta = 1 - \frac{C_{\text{downstream}}}{C_{\text{upstream}}} = 1 - \frac{C_{\text{cabin}}}{C_{\text{scuttle}}}, \quad (1)$$

where $C_{\text{cabin}}$ is the aerosol mass concentration measured in the cabin downstream of the cabin filter ($C_{\text{downstream}}$), and $C_{\text{scuttle}}$ is the aerosol mass concentration measured in the scuttle upstream of the cabin filter ($C_{\text{upstream}}$). The sampling points will be described below.

The PM10 DEKATI® cascade impactor was chosen for the gravimetric measurements because it enables the filtration efficiency of cabin filters to be estimated simultaneously for several aerosol fractions ($PM_1$, $PM_{2.5}$, $PM_{10}$) and is small enough to be transported by car. Aerosol sampling was carried out simultaneously in the cabin and the scuttle using two cascade impactors, each equipped with four quartz filters. These were operated with a diaphragm pump (QB1, Dadolab) at a flow rate of 30 L $min^{-1}$. The impactors collect size-fractionated aerosol: the fractions 1–2.5, 2.5–10, and $> 10$ µm (on quartz filters, Pall, 25 mm) and the fraction $< 1$ µm (on quartz filters, Whatman, 47 mm).

The aerosol mass concentration was determined by measuring the particle mass sampled on filters by the cascade

impactors. Quartz filters were pre-weighed and post-weighed with a Mettler Microbalance (Mettler Toledo XPR-2), which has an accuracy of 1 µg, after equilibrating for 24 h, in a room with controlled temperature and relative humidity (between 19 and 21 °C, with a relative humidity between 45 % and 50 %) according to standard NF EN 12341 2014. A generator for anti-static electricity was also used systematically during each weighing operation.

In parallel, two OPCs were used in the cabin and in the scuttle: (a) a GRIMM (Dust Monitor 1.108, Grimm Aerosol Technik) with mass distribution in cumulative mode for optical diameters between $> 0.23$ and $> 20$ µm (16 channels in total) and a flow rate of $1.2\,\mathrm{L\,min^{-1}}$ and (b) a DUSTTRAK 2 (Aerosol Monitor 8532, TSI®) with mass collection of $PM_{2.5}$ (0.3–2.5 µm) and a flow rate of $3\,\mathrm{L\,min^{-1}}$. For illustrative purposes, we sampled particles in-cabin with the Mini Particle Sampler® (MPS) (Ecomesure) (R'mili et al., 2013) on a transmission electron microscopy (TEM) grid with a flow rate of $0.3\,\mathrm{L\,min^{-1}}$ for 2–5 min. Then we analysed the grids using a JEOL JEM 1400 Plus transmission electron microscope to produce images and used the energy-dispersive X-ray (EDX) technique to determine the elemental composition of the particles.

### 2.2 Choice of the downstream sampling point

The downstream sampling point in the cabin was located downstream of the cabin filter in an area representative of passenger exposure at the respiratory level of the front-seat passenger. However, this sampling point is still far from the cabin filter. In the cabin, air dilution and air infiltration and exchange can occur (Harik et al., 2017). Consequently, particle concentrations at this point may be lower than just downstream of the cabin filter.

To determine whether this point could still be used for measurement downstream of the cabin filter, we relied on the literature. Grossmith et al. (2005) measured nitric oxide (NO) on the road at two sampling points: one at the front passenger seat level in the cabin and the other at the vehicle air inlet, closer to the cabin filter. The results showed that, over a sufficiently long period, both measurements provide the same NO concentration at the air inlet and in the cabin. Figure 1 (adapted from the report of Grossmith et al., 2005) represents the temporal evolution of the NO concentration measured simultaneously at the vehicle air inlet and in the cabin during a pollution episode. Two phenomena are observed: a "protection" period during which the NO concentration in the cabin is lower than at the air inlet and a "remanence" period when the NO concentration in the cabin persists even after the end of NO injection. Integrating the two peaks reveals an identical surface area, indicating that both measuring points were exposed to the same amount of pollutant throughout the measurement period. By analogy with NO, we expect the particles to behave in the same way and to be subject to the same dilution effect. The integration time of the cascade impactor is much longer (a few hours) than that shown in Fig. 1 (a few minutes). This ensures that almost all of the particles entering the cabin are measured. Therefore, the cabin sampling point enables the measurement of particles downstream of the cabin filter.

We also consider it to be the case that potential infiltration and dilution in the cabin would only have a minor impact on the measurement. Infiltration depends mainly on the size of the crack between doors and frames (Xu et al., 2010). Newer cars have better insulation and thus experience less infiltration of particles into the cabin (Fruin et al., 2011; Knibbs et al., 2010). The vehicle used for our tests was less than 2 years old. In addition, although ultrafine particles may infiltrate during an on-road trip, the literature shows that, at a medium fan setting, this infiltration is unaffected by driving speed (Lee et al., 2015). Therefore, by selecting this fan setting (see Sect. 2.3.2), we can assume that the contribution of ultrafine particles will be consistent across all tests, ensuring comparability. Furthermore, they contribute only slightly to the mass of the collected particles. Consequently, we assume that the downstream sampling point at the respiratory level is valid for evaluating cabin filters.

Regarding the project setup, we installed the DEKATI cascade impactor and the GRIMM OPC on a wooden structure positioned in place of the front seat (Fig. 2). No sampling line was used for both instruments. The inlets of the instruments were positioned at the respiratory level of a traveller. The DEKATI inlet was positioned higher than the GRIMM inlet to avoid interference between the two measurements. The diaphragm pump was connected to the cascade impactor and placed in the boot to avoid noise nuisance.

### 2.3 Choice of the upstream sampling point

#### 2.3.1 Design of sampling lines

To collect the particles upstream of the cabin filter, sampling lines were necessary to transfer the particles to the measuring instruments in the cabin (i.e. the cascade impactor DEKATI and the OPC GRIMM). There are two possible locations for the implementation of lines upstream of the cabin filter: on the outside of the vehicle or in the bonnet. The former offers the opportunity to collect data in traffic conditions. However, particles collected on the outside will not necessarily enter the bonnet until they reach the cabin filter. In addition, implementing lines implies that there will be particle losses during collection, which depend heavily on particle size. Larger particles are primarily affected by gravitational and inertial forces, whereas smaller particles are mainly affected by diffusional forces. These losses can occur during the inlet phase, when particles are drawn into the line, and during the transport phase, when particles pass through the line to the measuring instrument. When designing sampling lines, the challenge is to avoid these losses and to collect a representative sample, i.e. one whose characteristics (e.g.

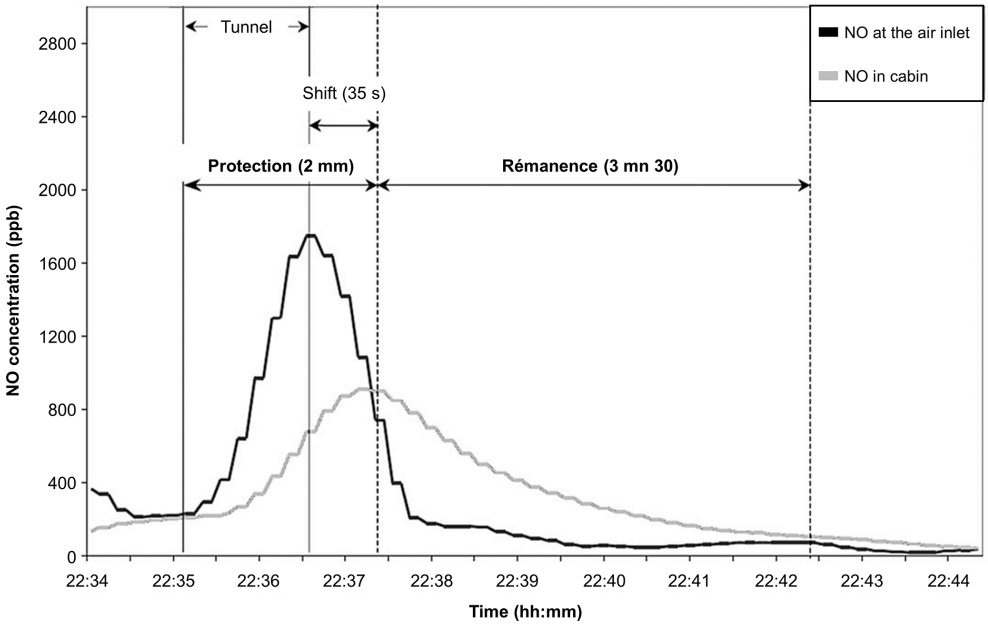



**Figure 1.** Time evolution of NO concentration at the air intake point and in the cabin (adapted from the report of Grossmith et al., 2005).

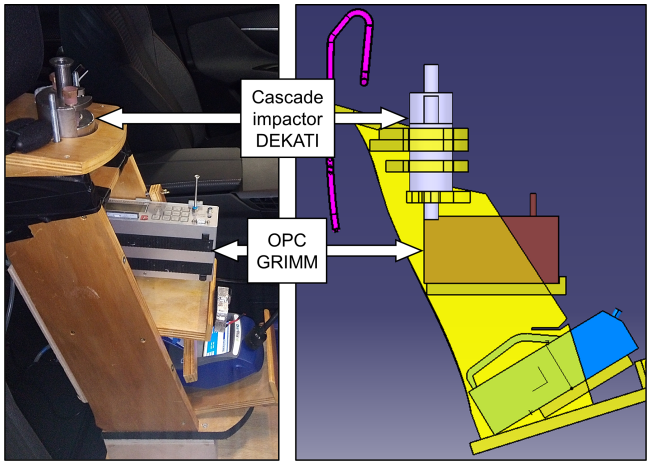



**Figure 2.** Installation of the instruments in the cabin. Left: photo. Right: scheme.

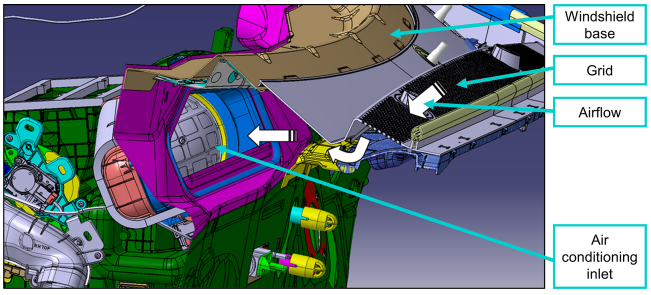



**Figure 3.** Scheme of the scuttle. The cabin air intake is located at the base of the windshield. It is then channelled to the cabin filter and the air conditioner before being distributed throughout the cabin.

particle concentration and size distribution) remain consistent between the sampled area and the measuring instrument. To collect a representative sample during the inlet phase, the sampling must be isokinetic (i.e. the velocities of the sampled and sampling streams are equal) and isoaxial (i.e. the inlets are positioned directly in the sampled stream) (Brockmann, 2011). In urban areas, traffic jams make it impossible to control the speed of vehicles. Therefore, isokinetic sampling in a traffic-congested situation requires either the design of an isokinetic probe (Heo et al., 2018) or the collection of particles in an area protected from speed fluctuations. The bonnet appears to be an area that is protected from wind fluctuations, and it is the area that is closest to the cabin filter. For these two reasons, we chose to place the measurement point in the bonnet as close to the cabin filter as possible in an area known as the "scuttle" (Fig. 3).

The scuttle is covered by a grid containing a closed section and an open section (Fig. 4). Air enters the scuttle through the open part of the grid and then passes through the "air inlet". We placed the inlets of the sampling line under the open section of the grid to face the wind. We drilled the scuttle to allow the sampling line to pass through it.

The sampling lines were designed following the recommendations of the literature (Brockmann, 2011), as described:

- Sampling lines should be as short as possible, with a constant diameter, to limit losses during transport.

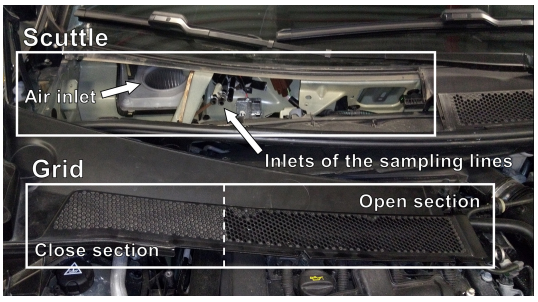



**Figure 4.** Photo of the scuttle. The grid was removed from the scuttle and placed on the bonnet for the photo.

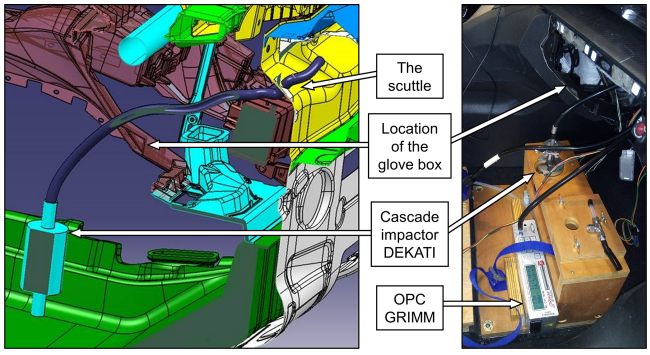



**Figure 5.** Installation of the sampling lines for the sampling upstream of the cabin filter. On the left: CAD of the line in the scuttle connected to the DEKATI in the cabin. On the right: picture of the installation of DEKATI and GRIMM in the cabin.

- Line diameters should be close to 1 cm to minimise deposition during the inlet phase.
- Sampling lines should be made of a special particulate sampling material (TSI, conductive silicone tubing for particle transport) to minimise possible electrostatic effects.

The parameters of the upstream sampling lines are listed in Table 1.

Figure 5 is a photo of the installation of the measuring instruments with the sampling lines in the cabin. Instruments were placed on a wooden structure on the floor. Sampling lines bend between the instruments and the location of the glove box to enter the scuttle. We removed the glove box to flatten the bend and limit particle losses during transport through the sampling lines.

Following the installation of the sampling lines, two parameters remained unknown:

- whether the isokinetic conditions were respected in the scuttle
- whether the line inlets sampled air directly from outside or from a recirculation zone in the scuttle.

Moreover, the sampling lines were not completely straight, forming a bend between the scuttle and the cabin (Fig. 5), which can lead to particle losses during the transport phase.

In order to determine the impact of these parameters on the sampling of $PM_1$, $PM_{2.5}$, and $PM_{10}$, we needed to establish the sampling efficiency of these three fractions. The sampling efficiency of the sampling lines can be calculated using the Eq. (2) (Brockmann, 2011):

$$\eta_{\text{sampling}} = \eta_{\text{inlet}} \eta_{\text{transport}}, \quad (2)$$

where $\eta_{\text{sampling}}$ is the overall efficiency of the sampling lines, $\eta_{\text{inlet}}$ is the inlet efficiency calculated with the sampling parameters (e.g. the wind velocity, the aspiration angle), and $\eta_{\text{transport}}$ is the transport efficiency calculated with the tubing parameters (e.g. the length, the diameter of the lines). The closer the sampling efficiency is to 1, the more representative the sample is. The sampling efficiency is calculated using multiple equations defined in the literature for calculating the inlet and transport efficiencies. This process can be time-consuming and prone to error. For this reason, we decided to consider the PLC software developed by von der Weiden et al. (2009), which combines the theoretical and empirical formulas established in the literature to estimate the sampling efficiency of a sampling line for multiple particle sizes.

Using this software requires determining all of the input data, i.e. the wind velocity and the airflow trajectory in the scuttle. The source of the sampled air (i.e. whether it is from outside the scuttle or from a recirculation area) also needs to be determined. A study of the scuttle was carried out to determine the missing input parameters using physical measurements (wind tunnel tests) and numerical simulations (CFD calculations, i.e. computational fluid dynamics calculations).

### 2.3.2 Aerodynamic characterisation of the scuttle

The objectives of the wind tunnel tests were (a) to identify the wind velocity in the scuttle and (b) to determine if it can be stable under certain conditions, which would allow us to control the sampling parameters.

Wind velocity was studied in the Jules Verne wind tunnel at the CSTB (Centre Scientifique et Technique du Bâtiment) in Nantes, France. Measuring 6000 $m^2$, the wind tunnel is used to study the dynamic and static behaviours of vehicles. It is equipped with six fans that produce airflow through four channels. Tests were conducted in the scuttle under the open part of the grid (Fig. 4) at various car speeds (0, 30, 80, and 130 $km\,h^{-1}$) and fan settings (fan speed levels). The fan airflow rate was set from "setting 0" (no ventilation) to "setting 4" (maximum airflow rate). For each configuration (one vehicle speed and one fan setting), the wind velocity was measured in the scuttle.

Figure 6 shows the evolution of wind velocity in the scuttle below the open section of the grid as a function of car speed and according to the five fan settings. This graph shows that

**Table 1.** The parameters of the sampling lines.

| Parameters | DEKATI (Gravimetry) | GRIMM (Optic) |
|---|---|---|
| Flow rate | 30 L min$^{-1}$ | 1.2 L min$^{-1}$ |
| Inner diameter | 8 mm | 8 mm |
| Bend | One bend of 20 cm and a straight line | One bend of 27 cm and a straight line |
| Lines length | 65.5 cm | 81.5 cm |

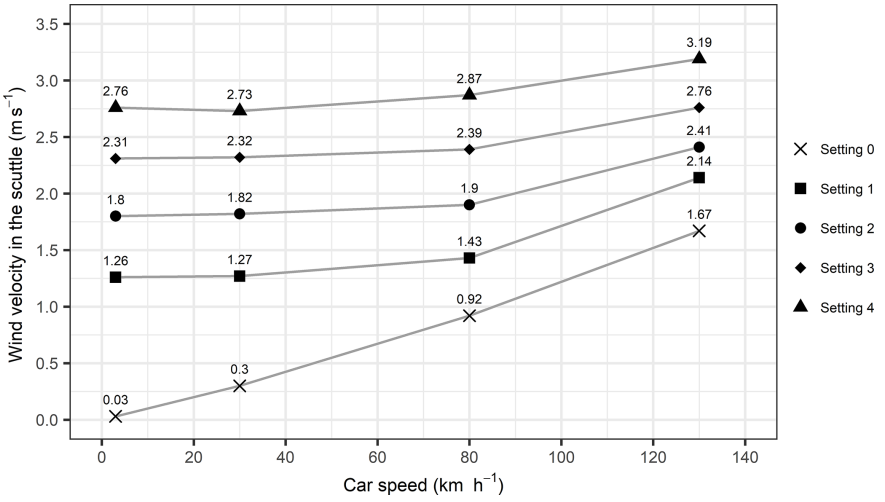



**Figure 6.** Evolution of car speed according to wind velocity in the scuttle and five fan settings (fan speed levels).

(i) wind velocity in the scuttle depends directly on the fan setting and (ii) wind velocity remains stable at speeds between 0 and 80 km h$^{-1}$ for fan settings 2 and 3. Therefore, for the tests, we selected setting 2 due to its stability. We therefore used an average wind velocity of 1.84 m s$^{-1}$ (the average of the three wind velocities measured in the scuttle at setting 2 between 0 and 80 km h$^{-1}$) as input for the PLC software. This selection limits the car speed to velocities between 0 and 80 km h$^{-1}$ during field trials.

The objectives of the CFD calculations were twofold: (i) to determine the trajectories of the airflow in the scuttle to verify that the line inlets face the wind (i.e. that sampling is isoaxial) and that the sample air comes directly from outside by determining the trajectories of the airflow in the scuttle and (ii) to determine the wind velocity numerically as a function of the fan setting.

CFD calculations were used to study the speed and trajectories of the airflow. CFD enables the simulation of fluid flow in an environment using a code that incorporates the laws of fluid mechanics (Navier–Stokes equations).

CFD calculations were performed using PowerFLOW Simulia software, which is used in the transport industry. This software can estimate speed fluctuations, for example, in an HVAC system. The scuttle was simulated using 12 levels of resolution and a fine mesh (with a maximum mesh size of 0.325 mm). Four configurations were simulated in the scuttle (Fig. 4): (a) a car travelling at 30 km h$^{-1}$ with fan setting 1, (b) a car travelling at 80 km h$^{-1}$ with fan setting 1, (c) a car travelling at 30 km h$^{-1}$ with fan setting 2, and (d) a car travelling at 80 km h$^{-1}$ with fan setting 2. The air flow rate is 110 kg h$^{-1}$ at fan setting 1 and 220 kg h$^{-1}$ at fan setting 2. A line was simulated in the area below the open part of the grid to represent the inlets of the DEKATI and GRIMM sampling-line inlets (Fig. 4).

Based on the simulations of the different configurations, wind velocities in configurations (a) and (b) are of the same order of magnitude (Fig. 7). The same was observed for configurations (c) and (d), with wind velocities greater than those for configurations (a) and (b). Therefore, wind velocity depends on the fan setting rather than the speed of the car (between 30 and 80 km h$^{-1}$). These results are consistent with those obtained in the wind tunnel, where similar observations were made. The wind velocities obtained through CFD calculations are of the same order of magnitude as the wind tunnel measurement results, with a maximum air velocity of 2 m s$^{-1}$ versus 1.43 m s$^{-1}$ at setting 1 according to CFD calculations and wind tunnel measurements, respectively, and a maximum air velocity of 3 and 1.9 m s$^{-1}$ at setting 2 according to CFD calculations and wind tunnel measurements, respectively.

According to the airflow trajectories simulated by CFD calculations, the sampling location is not in a recirculation zone. This means that the air sampled here comes directly from outside. At this point, the inlets of the DEKATI and

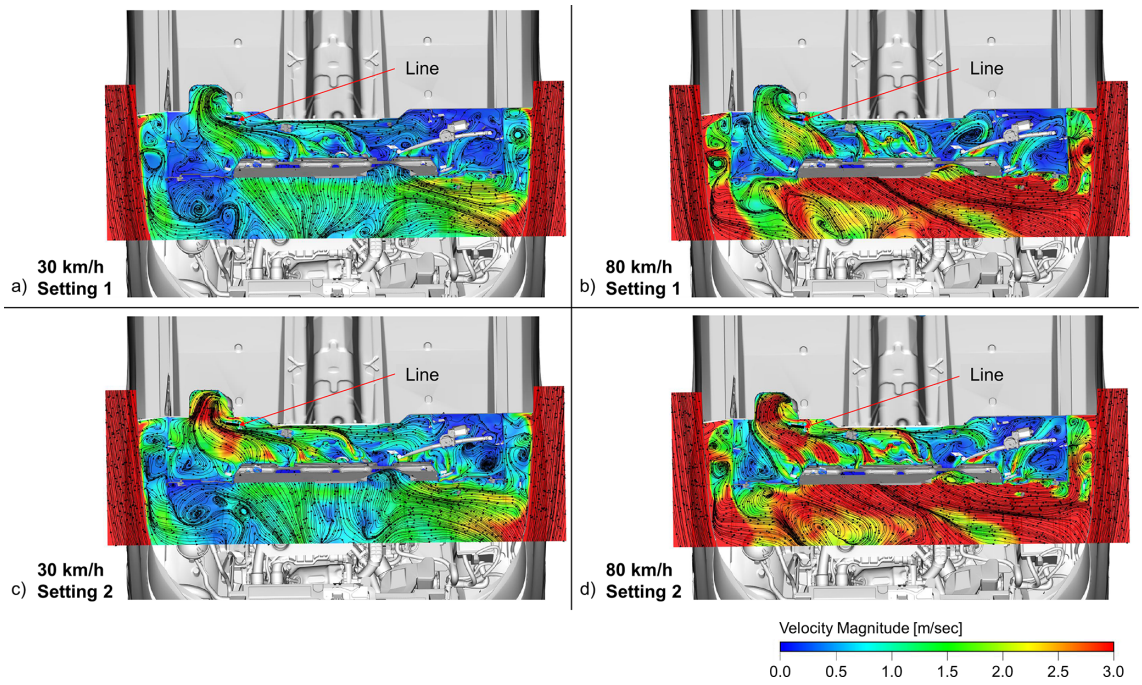



**Figure 7.** Airflow in the scuttle (view from top) for **(a)** fan setting 1 and a wind speed of 30 km h$^{-1}$, **(b)** fan setting 1 and a wind speed of 80 km h$^{-1}$, **(c)** fan setting 2 and a wind speed of 30 km h$^{-1}$, and **(d)** fan setting 2 and a wind speed of 80 km h$^{-1}$.

GRIMM lines can face the wind at an angle of 0°. The aspiration angle of the air at 0° was used as input data in the PLC software.

## 3 Results

In this section, we present some images of particles encountered on the road (Sect. 3.1) to illustrate what we sampled. For the evaluation of cabin filter performance, we focused on the DEKATI line as gravimetric measurements were preferred to obtain reliable results. First, we analysed its sampling efficiency (Sect. 3.2), and then we presented the sampling test in a moving car (Sect. 3.3). Next, we conducted a comparative analysis of the mass concentration of aerosols sampled simultaneously by DEKATI and the OPCs (Sect. 3.4) to evaluate the optical measurements. Finally, we assessed the filtration efficiency of cabin filters under real road conditions using DEKATI measurements (Sect. 3.5).

### 3.1 Illustration of particles encountered on the road

Figure 8 shows two images of particles sampled on TEM grids in the cabin and on the road with two different levels of zoom (10 µm in the left picture and 2 µm in the right picture). A dozen grids were analysed in total. The main species present on all grids were soot, foam-like particles, and black spots. Microscope analysis of particles in other road environments has also revealed the presence of these species (China et al., 2014; Hou et al., 2018; Xing et al., 2019). Soot was the predominant species on all of the grids (example on Fig. 8 left). They are composed solely of carbon and present as aggregates. The foam-like particles appear as light spots and are sensitive to the microscope beam, decomposing rapidly during analysis. The black spots are mainly composed of iron oxide, chromium, nickel, titanium, sulfur, potassium, and calcium.

### 3.2 Assessment of the sampling lines

The sampling efficiency (i.e. inlet and transport efficiency) of the lines in the scuttle was evaluated. The efficiency was calculated using PLC software and plotted as a function of particle aerodynamic diameter in Fig. 9. It shows that (i) above 0.2 µm, the sampling efficiency is slightly greater with the GRIMM than with the DEKATI, and (ii) the efficiency of the two sampling lines drops strongly around 1 µm for DEKATI and around 2 µm for GRIMM, with a decrease of half around 4 µm for DEKATI against 9 µm for the GRIMM.

Regarding the fractions of $PM_1$, $PM_{2.5}$, and $PM_{10}$ in particular, we considered it to be the case that the DEKATI line allows a quantitative sampling of $PM_1$, a satisfactory sampling of $PM_{2.5}$ (at 2.5 µm, the efficiency is 77 %), and an incomplete sampling of $PM_{10}$ (since the efficiency drops from 77 % to 0 % between 2.5 and 10 µm). Therefore, we considered the tests to be valid only for evaluating the $PM_1$ and $PM_{2.5}$ filtration under real road conditions.

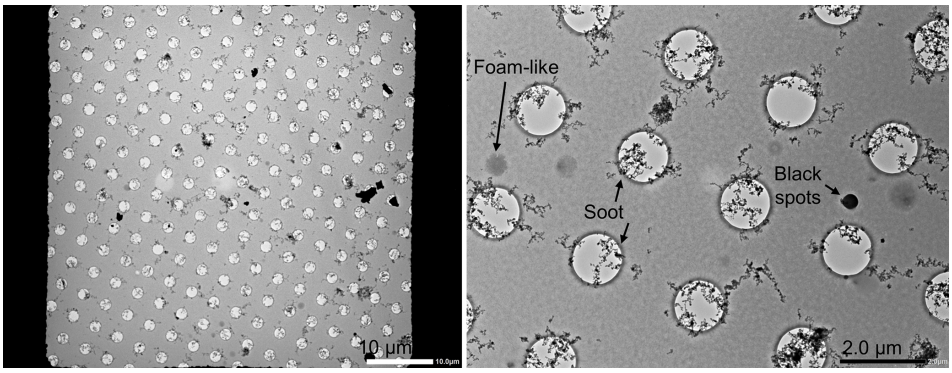



**Figure 8.** Illustration of particles on a TEM grid sampled in the cabin and on the road. On the left: with a scale of 10 µm. On the right: with a scale of 2 µm.

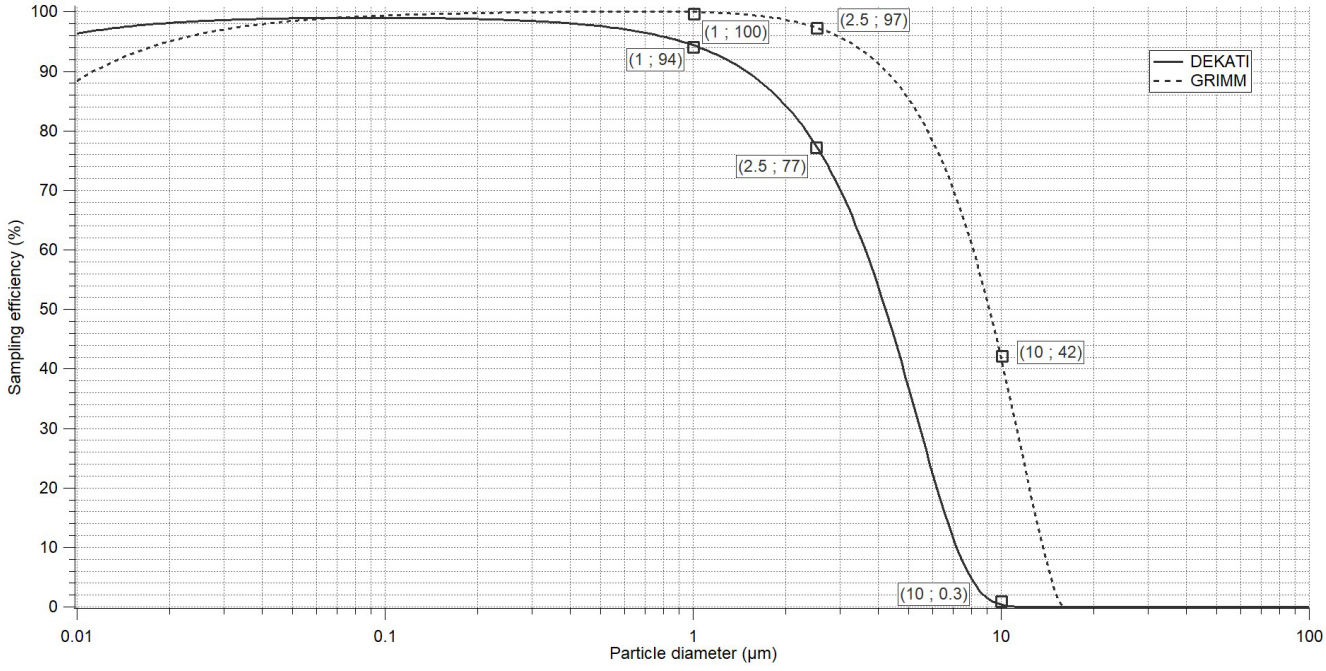



**Figure 9.** Sampling efficiency as a function of the particle diameter for the DEKATI and the GRIMM sampling lines set up in the scuttle.

### 3.3 Collection of experimental data

The vehicle, as described in Sect. 2, was used in two field campaigns in the Paris urban area in France. The first campaign took place in winter in February 2019 (in Paris and on the A86 freeway), and the second took place in summer in June–July 2019 (on the A86 freeway only), on weekdays only. All measurements were conducted under real driving conditions, at a maximum speed of 80 km h$^{-1}$, with ventilation set to level 2 and the windows closed. There were two to three passengers in the car during each test. During the winter campaign, the HVAC system in the car was set to 21 °C. The relative humidity was not measured. During the summer campaign, the air conditioning was switched on. The temperature and relative humidity were measured using a sensor. The average temperature was $28.1 \pm 2.1$ °C, with an average relative humidity of $37.3 \pm 4.4$ %. Gravimetric measurements were implemented in three configurations dedicated to evaluating the $PM_1$ and $PM_{2.5}$ filtration efficiency of two cabin filters labelled A and B, as well as in a situation without a cabin filter. The two cabin filters were new at the start of the first campaign and remained unchanged throughout the subsequent two campaigns. Two DEKATI samples were collected each day around 08:00 and 13:00 (sampling start times; UTC+1 for the first campaign, UTC+2 for the second campaign) for a period of 3 h. After the first campaign, we noticed that the mass of the indoor 1–2.5 µm fraction was sometimes below the limit of detection (LoD) for weighing. Therefore, in the second campaign, the DEKATI

filter for this fraction was changed after a longer sampling duration (i.e. after 6 h sampling instead of 3 h).

The sampling efficiency was calculated when both the in-scuttle and indoor measurements were above the LoD simultaneously (European Commission, 2013). On the first day of the first and second campaigns, one sample was discarded because the indoor particle concentration was higher than the in-scuttle concentration. We assume that particles accumulated in the cabin between the two campaigns because the vehicle was not used. In total, the filtration efficiency of $PM_1$ was determined 15 and 14 times for filters A and B, respectively, and 4 times in the case without a filter. The filtration efficiency of $PM_{2.5}$ was determined nine times for both filters A and B and four times in the case without a filter. The number of sampling periods, the resulting usable tests, and the situations allowing filtration efficiency calculation are summarised in Table 2 (for $PM_1$) and Table 3 (for $PM_{2.5}$), together with the associated sampling durations.

### 3.4 Comparison of gravimetric and optical measurements

The first step in processing the data was to compare the gravimetric and optical measurements. The aim is to identify a potential relationship between the measurements, which could pave the way for using an OPC (easier to use) to access the actual mass concentrations upstream and downstream of the filter. We considered the measurements on the same time step, averaging the OPC data over the DEKATI sampling intervals.

Out of the 33 sampling periods across the two campaigns, 48 $PM_{2.5}$ measurements (both indoor and in the scuttle) could be used to compare the two approaches (Tables 2 and 3). Of these, 31 were carried out during campaign 1, and 17 were carried out during campaign 2. The correlation matrix (Fig. 10) shows, at the intersection of the columns and rows, the following: (i) for two different devices, the correlations graphs (see Fig. 10b, c, and f) and their statistical parameters (see Fig. 10d, g, and h) for a given campaign and (ii) the distribution of data per campaign for the same device (see Fig. 10a, e, and i). The first campaign is shown in blue, and the second is shown in yellow.

As for GRIMM and DUSTTRAK, the regressions shown in Fig. 10f are statistically relevant, with a Pearson's correlation ($r$) around 0.9 and an associated significance level of $p < 0.001$ (Fig. 10h). The regression slopes are 0.7 and 0.9 for campaigns 1 and 2, respectively. However, the confidence envelopes associated with the regressions of each campaign overlap almost completely, indicating a highly reproducible correlation between the two devices over time. The difference between the two regressions could be attributed to the reduced concentration range of campaign 2 compared to that of campaign 1. Indeed, as the least-squares regression is sensitive to extreme values, the slopes differ slightly. As the two OPCs present a proportional signal, only the GRIMM–gravimetry comparison is studied here (Fig. 10b).

Figure 10b shows that a linear relationship can be derived between the concentration data obtained from DEKATI and GRIMM for each campaign. For both time periods, the Pearson's $r$ coefficient (Fig. 10d) is greater than 0.8 and is associated with a $p < 0.001$ significance level. However, the parameters of the relationship (slope and intercepts) differ significantly between the two campaigns. Since this finding could not be attributed to the instrument settings (calibration was checked before each campaign), we hypothesised that the biases induced by the optical methods used to calculate $PM_{2.5}$ mass concentrations varied according to the specificities of the sample. These biases could be due to changes in the composition of the particles, which affected their refractive index and density, and ultimately the conversion factor between number and mass concentrations. In our case, the change in season between campaigns is likely to have an impact on the nature of the sampled particles, for example, with a predominance of particles from heating in winter and more biogenic organic aerosols in summer (Favez et al., 2021; Zareba et al., 2024). If there were a purely affine relationship between optical particle size measurement (OPS) and gravimetry without intersection, it would be possible to use optical methods to evaluate filtration efficiency. However, the statistically significant, season-dependent bias between the gravimetric and optical methods in this study is incompatible with an accurate assessment of filtration efficiency under real road conditions.

### 3.5 Application of the gravimetric measurements on the road on two cabin filters

After validating the gravimetric measurements, we proceeded to the indoor and in-scuttle data for each configuration (i.e. filter A, filter B, no filter) from the DEKATI measurements. The distribution of $1 - \frac{C_{\text{cabin}}}{C_{\text{scuttle}}}$ (Eq. 1) for $PM_1$ and $PM_{2.5}$ was plotted for each configuration as boxplots in Fig. 11. These distributions document an initial cabin filter efficiency under real road conditions for filters A and B and provide information on the fraction of unavoidable particle reduction as they pass from the scuttle to the cabin, as well as measures uncertainties, for the tests without a cabin filter. The results allowed us to make several observations.

For the configuration without a cabin filter, the lowest value of $1 - \frac{C_{\text{cabin}}}{C_{\text{scuttle}}}$ is $-16\,\%$. This value seems surprising. It can be explained by non-significant differences in $PM_1$ $C_{\text{Cabin}}$ and $C_{\text{Scuttle}}$, with the following average concentrations and uncertainties: $16.6 \pm 1.7\,\mu g\,m^{-3}$ versus $14.3 \pm 1.6\,\mu g\,m^{-3}$, respectively. Without a cabin filter, the mass of particles in the cabin increased to a level comparable to that in the scuttle. The other values are higher than $0\,\%$ and reach a maximum of $26\,\%$ for $PM_1$ and of $42\,\%$ for $PM_{2.5}$. These values do not overlap with the filtration efficiency of filters A and B, except for one value for $PM_1$ and

**Table 2.** Summary of the number of $PM_1$ samples collected above the LoD in the vehicle (indoor) and in the scuttle, alongside the associated sampling duration and the number of situations in which filtration efficiency could be calculated.

| | $PM_1$: summary of the DEKATI data (with sampling duration) > LoD | | | | | | |
|---|---|---|---|---|---|---|---|
| | Field campaign no. 1 | | | Field campaign no. 2 | | | |
| | Indoor | In-scuttle | Filtration efficiency | Indoor | In-scuttle | Filtration efficiency | Total number of situations allowing filtration efficiency calculation |
| Filter A | 6 (3 h) | 6 (3 h) | 6 (3 h) | 9 (3 h) | 9 (3 h) | 9 (3 h) | 15 |
| Filter B | 7 (3 h) | 7 (3 h) | 7 (3 h) | 7 (3 h) | 7 (3 h) | 7 (3 h) | 14 |
| Without filter | 4 (3 h) | 4 (3 h) | 4 (3 h) | – | – | – | 4 |
| Total | 17 | 17 | 17 | 16 | 16 | 16 | |

**Table 3.** Summary of the number of $PM_{2.5}$ samples collected above the LoD in the vehicle (indoor) and in the scuttle, alongside the associated sampling duration and the number of situations in which filtration efficiency could be calculated.

| | $PM_{2.5}$: summary of the DEKATI data (with sampling duration) > LoD | | | | | | |
|---|---|---|---|---|---|---|---|
| | Field campaign no. 1 | | | Field campaign no. 2 | | | |
| | Indoor | In-scuttle | Filtration efficiency | Indoor | In-scuttle | Filtration efficiency | Total number of situations allowing filtration efficiency calculation |
| Filter A | 5 (3 h) | 6 (3 h) | 5 (3 h) | 4 (6 h) | 5 (6 h) | 4 (6 h) | 9 |
| Filter B | 5 (3 h) | 7 (3 h) | 5 (3 h) | 1 (3 h)<br>3 (6 h) | 1 (3 h)<br>3 (6 h) | 1 (3 h)<br>3 (6 h) | 9 |
| Without filter | 4 (3 h) | 4 (3 h) | 4 (3 h) | – | – | – | 4 |
| Total | 14 | 17 | 14 | 8 | 9 | 8 | |

two values for $PM_{2.5}$, demonstrating the effectiveness of the cabin filters.

Regarding the distribution of the two cabin filters, we find a close average efficiency (represented by a dotted line on boxplots) between them, both for $PM_1$ (54 % for filter A versus 53 % for filter B) and for $PM_{2.5}$ filtration (58 % for filter A versus 56 % for filter B). However, the values for filter A are more dispersed than for filter B for both $PM_1$ and $PM_{2.5}$. Given this result, we wondered whether it was due to the concentration of particles at the filter inlet, i.e. whether an increase in particle concentration in the scuttle affects filtration efficiency. To investigate this issue, we have plotted the $PM_1$ filtration efficiency results for filters A and B as a function of measured $PM_1$ concentrations in the scuttle in Fig. 12, using diamonds and circles for filters A and B, respectively.

The $x$ axis of Fig. 12 shows that filter A was tested over a wider concentration range than filter B (6.8 µg m$^{-3}$ to 64.1 µg m$^{-3}$ versus 20 µg m$^{-3}$ to 44.6 µg m$^{-3}$, respectively). To compare the filtration efficiency of both filters under the same conditions, we investigated their efficiency over the same range of particle concentrations in the scuttle (the grey area in Fig. 12). Then we plotted the boxplot distribution of the filtration efficiency (right side of Fig. 12) of both filters for this range. We found that, for the same range of particle concentrations in the scuttle, the $PM_1$ filtration efficiencies of the two filters remain close (51.4 % for filter A versus 52.7 % for filter B) but still more dispersed for filter A than for filter B (18.3 % to 76.5 % versus 35.5 % to 70.1 %). Based on these results, we can conclude that the concentration of $PM_1$ upstream of the cabin filter does not impact its filtration efficiency within the PM1 concentration range of 20 to 44.6 µg m$^{-3}$ in the scuttle. With the implementation of gravimetric measurements in a moving car, we have seen that it is possible to study the filtration efficiency of cabin filters under real road conditions and to add information on their dispersion.

## 4 Mechanisms responsible for the sampling losses

In Sect. 3.1, we quantified particle losses that occurred in the sampling line and found losses in the gravimetric (DEKATI) sampling line above 1 µm. While larger particles are less eas-

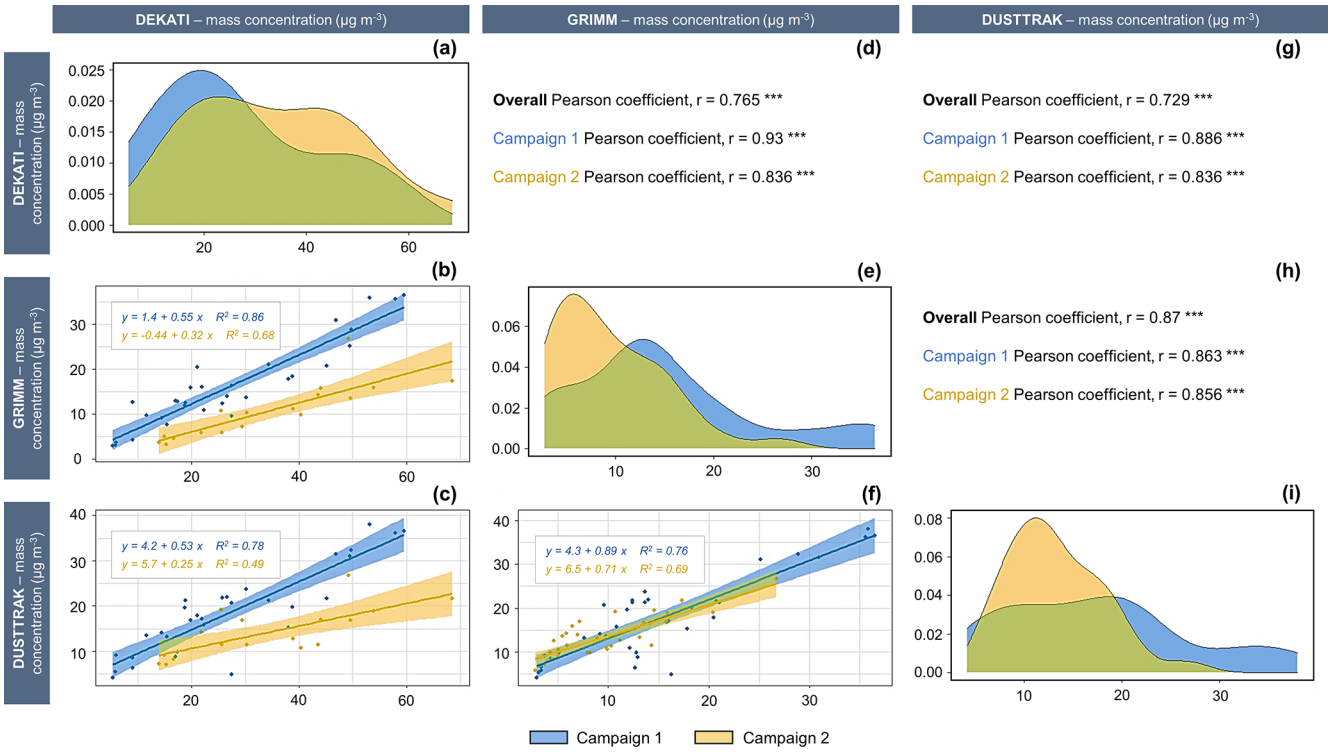



**Figure 10.** Correlation matrix of $PM_{2.5}$ measurement instruments for each campaign with (i) the weighted Pearson's correlation coefficient – $r$ – associated with its significance (*** for a significant correlation at 0.001 levels) and calculated with the Wilcoxon test on the upper triangular part **(d, g, h)**, (ii) the scatterplots on the lower triangular part **(b, c, f)**, and (iii) the density diagrams on the diagonal **(a, e, i)**. Campaign 1 is in blue, campaign 2 is in yellow, and the green part **(a, e, i)** is the intersection of the two distributions.

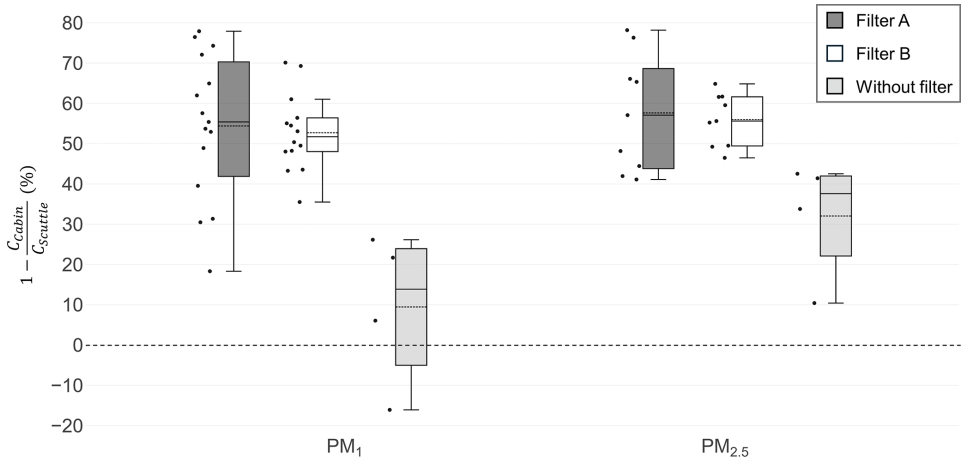



**Figure 11.** Distribution of the $PM_1$ and $PM_{2.5}$ filtration efficiency of filter A, filter B, and the case without filters with boxplots (the mean is represented by a dotted line, and the median, the 50th percentile, is represented by a solid line).

ily transported due to inertia, we investigated the sources of these phenomena to determine if losses in the DEKATI sampling line could be reduced. Using the PLC software, we identified the main mechanisms responsible for these losses during the inlet phase (Sect. 4.1) and during the transport phase (Sect. 4.2).

### 4.1 Improvement of the collection during the inlet phase

According to the PLC software calculations using the sampling-line parameters (Table 1), the airflow velocity in the DEKATI sampling line was 9.95 m s$^{-1}$, whereas the velocity in the scuttle was 1.84 m s$^{-1}$ according to the wind tunnel test results (see Sect. 2.3.1). Therefore, the airflow ve-

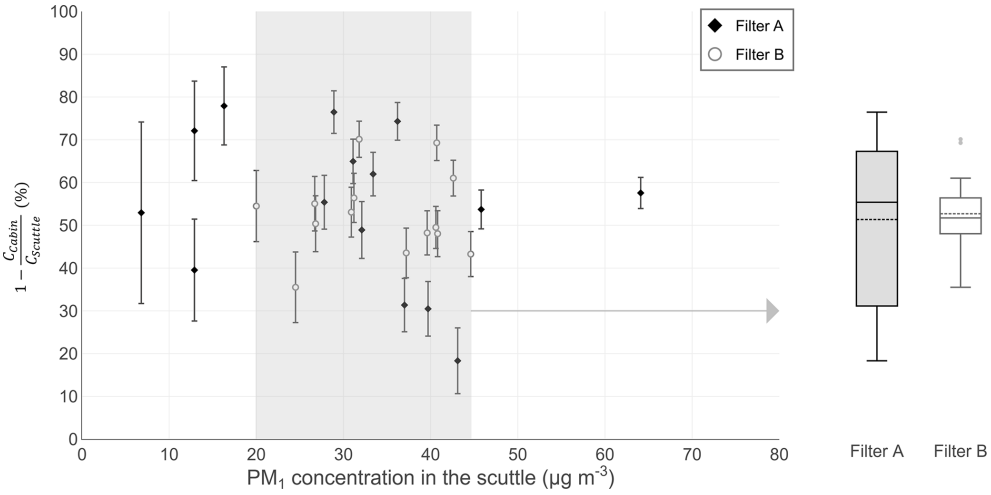



**Figure 12.** The $PM_1$ filtration efficiency of filters A and B, with expanded uncertainty, is shown as a function of the measured PM1 concentration in the scuttle. The expanded uncertainty was calculated by propagating the uncertainties and taking into account the filter weighting and sampled volume. The sampling efficiency distribution for measurements in the grey area is shown in the boxplots (the mean is represented by a dotted line, and the median, the 50th percentile, is represented by a solid line).

locity in the scuttle is much lower than in the DEKATI sampling line. The sampling is super-isokinetic, which results in an underestimation of the sampling of the largest particles.

To determine the consequences of non-isokinetic sampling on the DEKATI line, we ran the PLC software with a flow rate that allowed isokinetic sampling. Since the airflow velocity in the scuttle is 1.84 m s$^{-1}$, the flow rate of the DEKATI must be reduced from 30 to 5.5 L min$^{-1}$ to match this velocity in the line (the line diameter is 8 mm; see Table 1). We represented the sampling efficiency of the DEKATI line with this new flow rate in Fig. 13 (namely "simulation 5 L min$^{-1}$") and in the conditions of the experiment (namely "DEKATI 30 L min$^{-1}$").

Under isokinetic sampling conditions, the sampling efficiency (i.e. inlet and transport efficiency) is much higher for $PM_{10}$ (dotted line in Fig. 13). However, the flow rate of a cascade impactor cannot be changed because it determines the particle cutoff diameter. Thus, the inlet efficiency can be improved for the collection of the 2.5–10 µm fraction by (i) changing the cascade impactor model to a lower flow rate, (ii) increasing the air velocity in the scuttle by changing the ventilation setting, (iii) increasing the diameter of the sampling line to decrease the air flow velocity in the sampling line, and/or (iv) designing an isokinetic probe (Heo et al., 2018) for the speed range at which we want to carry out the measurements.

Using a model with a reduced flow rate instead of the cascade impactor would result in an increased collection time. Sampling $PM_{2.5}$ in the cabin required 360 min of collection time to ensure that the mass of particles between 1 and 2.5 µm was above the LoD. The larger the diameter of the particles, the more they are stopped by the cabin filter. Assuming a lower airflow velocity in the sampling line, the particle sampling collection time will exceed 360 min. This raises the question of how representative the time spent by travellers in their vehicles is. The second solution, using a fan at maximum speed to increase air velocity in the scuttle, will not represent traveller behaviour in all circumstances. For example, the fan is not pushed to its maximum during a winter trip. The third solution, using a line with a larger diameter for sampling, would involve drilling a larger hole in the scuttle to allow the line to pass through. Therefore, this solution seems to be the least restrictive in terms of not changing the test conditions (collection time and fan speed). The last solution requires designing an isokinetic probe, which will enable collection of the samples at different speeds. This method has previously been used to sample particles from a car through the window (Kam et al., 2012; Shirmohammadi et al., 2017). It could also be placed in the scuttle to measure the air just upstream of the cabin filter.

### 4.2 Improvement of the collection during the transport phase

In a second step, we identified the mechanisms responsible for particle losses during the transport phase. Figure 14 illustrates the transport efficiency of the DEKATI sampling line as a function of the particle diameter, along with a representation of the particle loss mechanisms. Each dashed line represents one mechanism, and the product of all of these mechanisms is the transport efficiency, represented by the solid line in Fig. 14. If we consider the transport efficiency of particles with a diameter of 10 µm, two main mechanisms are responsible for the losses: turbulent inertial deposition and inertial deposition in the line bend. This means that particles of this size cannot be transported along the line in the condi-

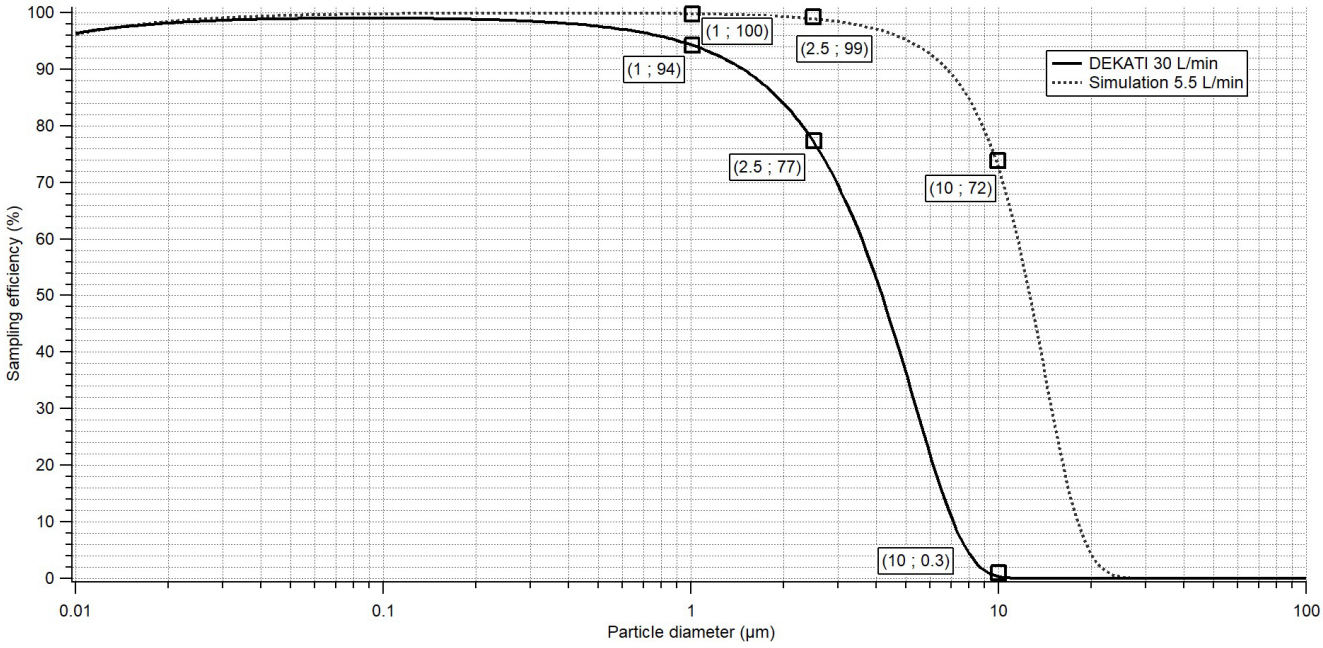



**Figure 13.** Sampling efficiency as a function of the particle diameter. This figure shows the sampling efficiency of the DEKATI instrument at a flow rate of 30 L $min^{-1}$ (solid line) and at a flow rate of 5.5 L $min^{-1}$ (dotted line). The latter flow rate was selected to reach the isokinetic sampling condition.

tions of this experiment. On the contrary, the sedimentation is responsible for only 5 % of the particles of 10 µm in the line (the transport efficiency is around 95 % for 10 µm in Fig. 14).

Although the bend in the sampling line was as straight as possible, the high air velocity in the small (8 mm) diameter sampling line may have contributed to these losses. This bend could not be avoided because it enabled the sampling line to enter the scuttle. However, this mechanism strongly impacts the collection of only one particle size fraction (2.5–10 µm). Furthermore, we found that the main cause of particle loss is non-isokinetic sampling rather than particle deposition in the bends (Fig. 13).

Therefore, different mechanisms are responsible for particle losses during sampling. The super-isokinetic sampling condition results in the highest losses. A sampling line was used for the scuttle measurement but not for the cabin measurement. The aerosol concentration measurement in the scuttle was not corrected in the filter efficiency calculation. Consequently, the filtration efficiency results (Figs. 11 and 12) were underestimated. In the future, correcting the scuttle measurements could provide a more accurate filtration efficiency result.

## 5 Discussion

This study estimated the filtration efficiency of two cabin filters for $PM_1$ and $PM_{2.5}$ under real-road conditions. The main limitation of the on-road study is that field conditions (e.g. weather, traffic) can vary during measurements and consequently influence filtration efficiency (see Sect. 1) (He et al., 2016). Furthermore, the properties of the particles can be altered by these changes, which then affects their filtration. For example, Bukowiecki et al. (2002) estimated that, due to higher relative humidity, particle size was 10 % larger on suburban and rural roads at night than during the day. Thus, neither the content of the future database, the variability of the field conditions encountered, nor their impact on filtration efficiency is guaranteed. Consequently, designing an experiment to compare the performance of two different cabin air filters under the same on-road conditions is complex. Additionally, on-road measurements are more expensive than laboratory studies, making parametric studies with a high degree of repeatability challenging to envision. Laboratory tests ensure repeatable results since they are carried out under stable and controlled conditions. They also make it possible to study the effect of a specific parameter on the filter's performance, such as its age, thickness, weight, or pore size (Lim et al., 2018; Shim et al., 2022). Therefore, road tests complement laboratory studies but are hardly self-fulfilling.

The on-road measurements have the advantage of filling a gap that the standards do not address. During laboratory tests, standard particles are used (e.g. Arizona desert dust in the standard ISO 12103-1), which are not representative of all particles present in urban air. Moreover, standards do not cover the full range of particle sizes (e.g. the standard ISO/TS 11155-1 covers particles larger than 0.3 µm), while studies have shown that ultrafine particles (smaller than 0.1 µm in diameter) are present in the cabin (e.g. the average con-

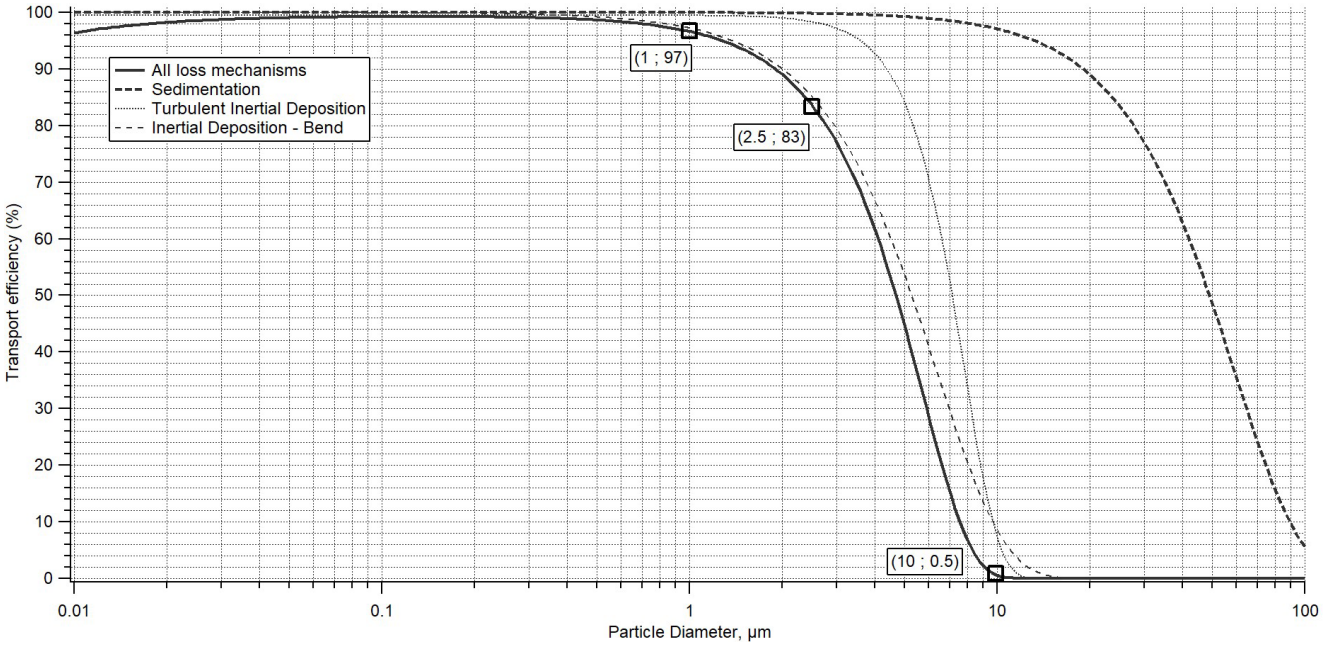



**Figure 14.** Transport efficiency as a function of the particle diameter for the DEKATI instrument, showing the particle loss mechanisms.

centration of ultrafine particles in the cabin is greater than $10^4$ particles $cm^{-3}$ in Asia, Europe, and the USA) and have a specific impact on health (e.g. increase in inflammation, cardiovascular mortality) (Kumar et al., 2018; Qi et al., 2008). For all of these reasons, it is necessary to be able to determine the filter efficiency under realistic conditions as well.

In this paper, we proposed an original approach for the evaluation of cabin filters on the road. We used a reference method, gravimetry, to determine the mass concentration of particles. Our comparison of gravimetric and OPC measurements (see Sect. 3.4) showed that, while the two types of measurement correlated well, a correction factor had to be applied to obtain the true value. This result was not surprising because the OPCs are calibrated using spherical latex particles that do not represent particles in ambient air. Implementing gravimetry requires human resources (more than 300 filters were weighted during this project) and financial resources (for the filters, the weighing room, and the precision scale). Hence, it is not accessible to everyone. However, these results confirm the need to use it on road since mass concentration is not approximated. If a pre-campaign of measurements is conducted at the start of each batch of campaign to determine a seasonal correction model, OPCs can be used instead of gravimetry to determine the mass concentration of particles. Nonetheless, conditions in the ambient air can change rapidly (e.g. work construction, agricultural trade, dust event, fire), rendering this factor invalid. OPCs still stay useful as gravimetry does not provide filtration efficiency by particle size or real-time measurements. Therefore, we recommend implementing both methods simultaneously since they complement each other.

The methodology described in this paper has provided insights into how the filters perform under real-road conditions. We saw that the filtration efficiency of a cabin filter can vary considerably under real conditions, e.g. the $PM_{2.5}$ filtration efficiency ranged from 41.1 % to 78.2 % for filter A and from 46.5 % to 61.6 % for filter B. These results are in line with the literature, where such discrepancies have already been observed, e.g. from 50.3 % to 93.2 % with a filter used on the road in China (Yin et al., 2023). However, the instruments used and the locations of the measurements differ from one study to another. This makes comparisons difficult because there is currently no harmonised test procedure. Hence, we aimed to apply the methodology to other vehicles and filters and then compared the results.

To reach this step, we recommend considering the following limitations:

- We used a sampling line in this area and characterised its particle losses with the PLC software. However, we did not experimentally validate the results of the calculation. This is an important step to accurately assess the performance of the cabin filters. To address this question, the sampling line could be reproduced in laboratory, and the losses during transport could be quantified.

- This protocol is not universal, and the methodology must be adapted to the vehicle being tested. To do this, the airflow in the HVAC system must be studied. We did wind tunnel measurements and CFD calculations in this paper. Other methods can also be used for this purpose. For example, tracer smoke can be injected into the vehicle to identify airflow patterns and to locate dead zones.

- To improve the collection of particles upstream of the cabin filter, isokinetic sampling must be guaranteed (see the recommendation in Sect. 4.1). This will ensure an accurate assessment of cabin filter performance.
- If the study does not relate to passenger exposure, the downstream sampling location must be placed closer to the cabin filter. The current measurement point was located at the respiratory level of a traveller and therefore was not as close as possible to the air inlet in the cabin. In the future, a more specific sampling point downstream of the filter could be developed for the evaluation of cabin filters only, potentially being less subject to dilution and infiltration that may occur in the cabin.
- To prevent particles from entering the vehicle through the window frames while driving, windows can be sealed with tape (Liu et al., 2011).
- The conditions of the experiments must be tracked, such as temperature, relative humidity, air conditioning, traffic conditions, and the number of passengers, as these could influence the results.

## 6 Conclusion and perspectives

We conducted gravimetric on-road measurements for evaluating cabin filters as a complement to laboratory studies. For this purpose, two sampling points were designed: one upstream of the cabin filter in the scuttle and one downstream of the cabin filter on the front passenger seat. An aeraulic study (wind tunnel measurements, CFD calculations) of the scuttle (an area in the bonnet) shows that it represents an interesting zone for measuring pollutants because (i) it is in the airflow path through the cabin filter and (ii) the wind speed fluctuates minimally in this area under certain ventilation conditions (setting 2 in this study), allowing for stable testing conditions. A sampling line was used to collect the particles in the scuttle. The PLC software (von der Weiden et al., 2009) was used to evaluate its sampling efficiency. The results show that the sampling efficiency is greater than 94 % for $PM_1$ and greater than 77 % for $PM_{2.5}$. However, the sampling efficiency of the line is greatly reduced for particles larger than 2.5 µm in diameter. This means that the filtration efficiency of cabin filters for $PM_{10}$ cannot be evaluated. The filtration efficiency of two different filters was assessed in a moving car in an urban area for the $PM_1$ and $PM_{2.5}$ fractions. The average filtration efficiency was similar for both filters (e.g. 54 % and 53 % filtration efficiency for $PM_1$ in 15 and 14 tests, respectively), but the results were more scattered for one filter than for the other.

A comparison should be made between these results and the evaluation of the same filters by a standard in a laboratory. Such a comparison would highlight discrepancies between laboratory and on-road measurements and provide insight into how the filters behave depending on the road conditions. For example, Heo et al. (2022) found a decrease in the filtration efficiency of one filter from 87 % to 58 % when comparing laboratory and on-road measurement. They suggested that the solid–liquid nature of on-road aerosols, as opposed to the standard of only solid aerosols, accelerates the degradation of filtration efficiency.

These tests can be performed on another vehicle, provided that the sampling conditions at the scuttle and along the sampling line are properly evaluated (e.g. using PLC software). This will allow filter manufacturers to test the filtration efficiency of any type of cabin filter under different conditions, such as traffic, vehicle type, and weather conditions. Additionally, the variation in cabin filter performance over time should be studied to determine when filters need to be changed to continue protecting travellers. For example, the impact of clogging on filtration efficiency should be investigated.

**Data availability.** Data are available on the online Zenodo data repository: https://doi.org/10.5281/zenodo.22671117 (Delater et al., 2026).

**Author contributions.** A. Delater: writing (original draft), data curation, investigation, methodology, visualisation. S. Fable: investigation, conceptualisation. B. Berthelot: writing (original draft, review and editing), data curation, visualisation. C. Raventos: formal analysis. J. Queron: funding acquisition, supervision, writing (review and editing). I. Coll: writing (original draft, review and editing), validation. O. Le Bihan: conceptualisation, project administration, supervision, validation, writing (review and editing).

**Competing interests.** The contact author has declared that none of the authors has any competing interests.

**Disclaimer.** Publisher's note: Copernicus Publications remains neutral with regard to jurisdictional claims made in the text, published maps, institutional affiliations, or any other geographical representation in this paper. The authors bear the ultimate responsibility for providing appropriate place names. Views expressed in the text are those of the authors and do not necessarily reflect the views of the publisher.

**Acknowledgements.** We thank our partner on the project, a car manufacturer. The QABINE and QABINE2 (Qualité de l'Air dans les haBItacles eN déplacEment) projects were supported under the CORTEA programme. Finally, the authors want to thank Olivier Aguerre-Chariol for the TEM analysis, Céline Ferret for her valuable advice regarding filter weighing, and Thomas Audoux for his assistance and guidance during the revision of this article.

**Financial support.** This research has been supported by the Agence de l'Environnement et de la Maîtrise de l'Energie (grant no. 1766C0004).

**Review statement.** This paper was edited by Christof Asbach and reviewed by two anonymous referees.

## References

Alves, C. A., Vicente, E. D., Vicente, A. M. P., Rienda, I. C., Tomé, M., Querol, X., and Amato, F.: Loadings, chemical patterns and risks of inhalable road dust particles in an Atlantic city in the north of Portugal, Sci. Total Environ., 737, 139596, https://doi.org/10.1016/j.scitotenv.2020.139596, 2020.

Amato, F., Pandolfi, M., Moreno, T., Furger, M., Pey, J., Alastuey, A., Bukowiecki, N., Prevot, A. S. H., Baltensperger, U., and Querol, X.: Sources and variability of inhalable road dust particles in three European cities, Atmos. Environ., 45, 6777–6787, https://doi.org/10.1016/j.atmosenv.2011.06.003, 2011.

Brockmann, J. E.: Aerosol Transport in Sampling Lines and Inlets, in: Aerosol Measurement, 68–105, https://doi.org/10.1002/9781118001684.ch6, 2011.

Bukowiecki, N., Dommen, J., Prévôt, A. S. H., Richter, R., Weingartner, E., and Baltensperger, U.: A mobile pollutant measurement laboratory – measuring gas phase and aerosol ambient concentrations with high spatial and temporal resolution, Atmos. Environ., 36, 5569–5579, https://doi.org/10.1016/S1352-2310(02)00694-5, 2002.

China, S., Salvadori, N., and Mazzoleni, C.: Effect of Traffic and Driving Characteristics on Morphology of Atmospheric Soot Particles at Freeway On-Ramps, Environ. Sci. Technol., 48, 3128–3135, https://doi.org/10.1021/es405178n, 2014.

Delater, A., Fable, S., Berthelot, B., Raventos, C., Queron, J., Coll, I., and Le Bihan, O.: Assessment of cabin filtration efficiency: contribution to an on-road methodology, Zenodo [data set], https://doi.org/10.5281/zenodo.22671117, 2026.

DIN 71460-1: Road vehicles – Air filters for motor passenger compartments – Part 1: Test for particulate filtration, Deutsches Institut für Normung e.V., https://doi.org/10.31030/9703800, 2006.

Dons, E., Temmerman, P., Van Poppel, M., Bellemans, T., Wets, G., and Int Panis, L.: Street characteristics and traffic factors determining road users' exposure to black carbon, Sci. Total Environ., 447, 72–79, https://doi.org/10.1016/j.scitotenv.2012.12.076, 2013.

European Commission: Commission Implementing Decision laying down rules for Directives 2004/107/EC and 2008/50/EC of the European Parliament and of the Council as regards the reciprocal exchange of information and reporting on ambient air (Decision 2011/850/EU), https://eur-lex.europa.eu/eli/dec_impl/2011/850/oj/ (last access: 5 November 2026), 2013.

European Environment Agency: Air pollution in Europe: 2024 reporting status under the National Emission reduction Commitments Directive, https://www.eea.europa.eu/publications/national-emission-reduction-commitments-directive-2024 (last access: 27 February 2025), 2024a.

European Environment Agency: Europe's air quality status, https://www.eea.europa.eu//publications/europes-air-quality-status-2024 (last access: 27 February 2025), 2024b.

Favez, O., Weber, S., Petit, J.-E., Alleman, L. Y., Albinet, A., Riffault, V., Chazeau, B., Amodeo, T., Salameh, D., Zhang, Y., Srivastava, D., Samaké, A., Aujay-Plouzeau, R., Papin, A., Bonnaire, N., Boullanger, C., Chatain, M., Chevrier, F., Detournay, A., Dominik-Sègue, M., Falhun, R., Garbin, C., Ghersi, V., Grignion, G., Levigoureux, G., Pontet, S., Rangognio, J., Zhang, S., Besombes, J.-L., Conil, S., Uzu, G., Savarino, J., Marchand, N., Gros, V., Marchand, C., Jaffrezo, J.-L., and Leoz-Garziandia, E.: Overview of the French Operational Network for In Situ Observation of PM Chemical Composition and Sources in Urban Environments (CARA Program), Atmosphere, 12, 207, https://doi.org/10.3390/atmos12020207, 2021.

Fruin, S. A., Hudda, N., Sioutas, C., and Delfino, R. J.: Predictive Model for Vehicle Air Exchange Rates Based on a Large, Representative Sample, Environ. Sci. Technol., 45, 3569–3575, https://doi.org/10.1021/es103897u, 2011.

Gan, W. Q., Koehoorn, M., Davies, H. W., Demers, P. A., Tamburic, L., and Brauer, M.: Long-Term Exposure to Traffic-Related Air Pollution and the Risk of Coronary Heart Disease Hospitalization and Mortality, Environ. Health Perspect., 119, 501–507, https://doi.org/10.1289/ehp.1002511, 2011.

Greenwald, R., Bergin, M. H., Yip, F., Boehmer, T., Kewada, P., Shafer, M. M., Schauer, J. J., and Sarnat, J. A.: On-Roadway In-Cabin Exposure to Particulate Matter: Measurement Results Using Both Continuous and Time-Integrated Sampling Approaches, Aerosol Sci. Tech., 48, 664–675, https://doi.org/10.1080/02786826.2014.912745, 2014.

Grossmith, A., Le Bihan, O., Gouriou, F., Reynaud, M., Aujay, R., and Godet, Y.: Caractérisation de l'exposition en habitacle automobile, Rapport d'étude no. 66354, INERIS, Verneuil-en-Halatte, France, 2005.

GRPE-70-09-Rev.1: IWG on VIAQ: Informal document, Terms of reference and rules of procedure for the Informal Working Group on Vehicle Interior Air Quality (VIAQ), GRPE-70-09-Rev.1, UNECE, https://unece.org/70th-session-4 (last access: 28 October 2026), 2015.

GRPE-81-09: Informal document, Terms of reference and rules of procedure for the Informal Working Group on Vehicle Interior Air Quality – Third stage, UNECE, https://unece.org/81st-session-4 (last access: 28 October 2026), 2020.

Harik, G., El-Fadel, M., Shihadeh, A., Alameddine, I., and Hatzopoulou, M.: Is in-cabin exposure to carbon monoxide and fine particulate matter amplified by the vehicle's self-pollution potential? Quantifying the rate of exhaust intrusion, Transp. Res. Part Transp. Environ., 54, 225–238, https://doi.org/10.1016/j.trd.2017.05.009, 2017.

He, X., Brem, B. T., Bahk, Y. K., Kuo, Y.-Y., and Wang, J.: Effects of relative humidity and particle type on the performance and service life of automobile cabin air filters, Aerosol Sci. Tech., 50, 542–554, https://doi.org/10.1080/02786826.2016.1167832, 2016.

Heo, K. J., Noh, J. W., Lee, B. U., Kim, Y., and Jung, J. H.: Comparison of filtration performance of commercially available automotive cabin air filters against various airborne pollutants, Build. Environ., 161, 106272, https://doi.org/10.1016/j.buildenv.2019.106272, 2019.

Heo, K. J., Noh, J. W., Kim, Y., and Jung, J. H.: Comparison of the service life of an automotive cabin air filter under dust loading conditions of the laboratory environment and on-road driving, J. Aerosol Sci., 162, 105972, https://doi.org/10.1016/j.jaerosci.2022.105972, 2022.

Heo, N.-G., Lim, J.-H., Lee, J.-W., Lee, J.-S., Yook, S.-J., and Ahn, K.-H.: Development of a Sampling Probe for Representative Sampling of PM at Freestream Velocities in the Range from 0 to 300 km h−1, J. Atmos. Ocean. Tech., 35, 727–738, https://doi.org/10.1175/JTECH-D-17-0158.1, 2018.

Hinds, W. C.: Physical and Chemical Processes in Aerosol Systems, in: Aerosol Measurement, John Wiley & Sons, Ltd, 31–40, https://doi.org/10.1002/9781118001684.ch3, 2011.

Hou, C., Shao, L., Hu, W., Zhang, D., Zhao, C., Xing, J., Huang, X., and Hu, M.: Characteristics and aging of traffic-derived particles in a highway tunnel at a coastal city in southern China, Sci. Total Environ., 619–620, 1385–1393, https://doi.org/10.1016/j.scitotenv.2017.11.165, 2018.

ISO 12103-1: Road vehicles – Test contaminants for filter evaluation – Part 1: Arizona test dust, International Organization for Standardization, https://www.iso.org/standard/85949.html? (last access: 5 November 2026), 2016.

ISO/TS 11155-1: Road vehicles – Air filters for passenger compartments – Part 1: Test for particulate filtration, International Organization for Standardization, https://www.iso.org/standard/34308.html? (last access: 5 November 2026), 2001.

Kam, W., Liacos, J. W., Schauer, J. J., Delfino, R. J., and Sioutas, C.: Size-segregated composition of particulate matter (PM) in major roadways and surface streets, Atmos. Environ., 55, 90–97, https://doi.org/10.1016/j.atmosenv.2012.03.028, 2012.

Knibbs, L. D., De Dear, R. J., and Morawska, L.: Effect of Cabin Ventilation Rate on Ultrafine Particle Exposure Inside Automobiles, Environ. Sci. Technol., 44, 3546–3551, https://doi.org/10.1021/es9038209, 2010.

Kumar, P., Patton, A. P., Durant, J. L., and Frey, H. C.: A review of factors impacting exposure to PM2.5, ultrafine particles and black carbon in Asian transport microenvironments, Atmos. Environ., 187, 301–316, https://doi.org/10.1016/j.atmosenv.2018.05.046, 2018.

Lee, E. S. and Zhu, Y.: Application of a High-Efficiency Cabin Air Filter for Simultaneous Mitigation of Ultrafine Particle and Carbon Dioxide Exposures Inside Passenger Vehicles, Environ. Sci. Technol., 48, 2328–2335, https://doi.org/10.1021/es404952q, 2014.

Lee, E. S., Stenstrom, M. K., and Zhu, Y.: Ultrafine particle infiltration into passenger vehicles. Part II: Model analysis, Transp. Res. Part Transp. Environ., 38, 144–155, https://doi.org/10.1016/j.trd.2014.11.005, 2015.

Lim, T. H., Yeo, S. Y., and Lee, S. H.: Multidirectional evaluations of a carbon air filter to verify their lifespan and various performances, J. Aerosol Sci., 126, 205–216, https://doi.org/10.1016/j.jaerosci.2018.09.009, 2018.

Liu, S. S., Wang, R., and Xiao, H. X.: Design and Compare of the Three Cabin Air Fiber Filter Testing Methods for Removal of PM2.5, Adv. Mater. Res., 197–198, 1515–1519, https://doi.org/10.4028/www.scientific.net/AMR.197-198.1515, 2011.

NF EN 12341: Ambient air – Standard gravimetric measurement method for the determination of the PM10 or PM2,5 mass concentration of suspended particulate matter, ICS: 13.040.20, AFNOR, Association française de normalisation, https://www.boutique.afnor.org/fr-fr/norme/nf-en-12341/fa186364/351830? (last access: 5 November 2026), 2023.

Qi, C., Stanley, N., Pui, D. Y. H., and Kuehn, T. H.: Laboratory and On-Road Evaluations of Cabin Air Filters Using Number and Surface Area Concentration Monitors, Environ. Sci. Technol., 42, 4128–4132, https://doi.org/10.1021/es703216c, 2008.

R'mili, B., Le Bihan, O. L. C., Dutouquet, C., Aguerre-Charriol, O., and Frejafon, E.: Particle Sampling by TEM Grid Filtration, Aerosol Sci. Tech., 47, 767–775, https://doi.org/10.1080/02786826.2013.789478, 2013.

Robert, B., Ana, S., Adina, B. B., and Corneliu, B. B.: Comparative study of filtration parameters depending on the nature of the filter material, Mater. Today Proc., 78, 343–347, https://doi.org/10.1016/j.matpr.2023.02.124, 2023.

Shim, E., Noh, J., and Kim, Y.: Development and Performance Evaluation of Polytetrafluoroethylene-Membrane-Based Automotive Cabin Air Filter, ACS Omega, 7, 43738–43746, https://doi.org/10.1021/acsomega.2c04758, 2022.

Shirmohammadi, F., Wang, D., Hasheminassab, S., Verma, V., Schauer, J. J., Shafer, M. M., and Sioutas, C.: Oxidative potential of on-road fine particulate matter (PM2.5) measured on major freeways of Los Angeles, CA, and a 10-year comparison with earlier roadside studies, Atmos. Environ., 148, 102–114, https://doi.org/10.1016/j.atmosenv.2016.10.042, 2017.

Sinharay, R., Gong, J., Barratt, B., Ohman-Strickland, P., Ernst, S., Kelly, F. J., Zhang, J., Collins, P., Cullinan, P., and Chung, K. F.: Respiratory and cardiovascular responses to walking down a traffic-polluted road compared with walking in a traffic-free area in participants aged 60 years and older with chronic lung or heart disease and age-matched healthy controls: a randomised, crossover study, Lancet Br. Ed., 391, 339–349, https://doi.org/10.1016/S0140-6736(17)32643-0, 2018.

von der Weiden, S.-L., Drewnick, F., and Borrmann, S.: Particle Loss Calculator – a new software tool for the assessment of the performance of aerosol inlet systems, Atmos. Meas. Tech., 2, 479–494, https://doi.org/10.5194/amt-2-479-2009, 2009.

Wang, C., Liu, J., He, M., Xu, J., and Liao, H.: Investigating the filtration performance and service life of vehicle cabin air filters in China, Environ. Int., 190, 108939, https://doi.org/10.1016/j.envint.2024.108939, 2024.

Wei, D., Nielsen, F., Ekberg, L., Löfvendahl, A., Bernander, M., and Dalenbäck, J.-O.: PM2.5 and ultrafine particles in passenger car cabins in Sweden and northern China – the influence of filter age and pre-ionization, Environ. Sci. Pollut. Res., 27, 30815–30830, https://doi.org/10.1007/s11356-020-09214-0, 2020.

Xing, J., Shao, L., Zhang, W., Peng, J., Wang, W., Hou, C., Shuai, S., Hu, M., and Zhang, D.: Morphology and composition of particles emitted from a port fuel injection gasoline vehicle under real-world driving test cycles, J. Environ. Sci., 76, 339–348, https://doi.org/10.1016/j.jes.2018.05.026, 2019.

Xu, B., Liu, S., and Zhu, Y.: Ultrafine particle penetration through idealized vehicle cracks, J. Aerosol Sci., 41, 859–868, https://doi.org/10.1016/j.jaerosci.2010.05.005, 2010.

Xu, B., Liu, S., Liu, J., and Zhu, Y.: Effects of Vehicle Cabin Filter Efficiency on Ultrafine Particle Concentration Ratios Measured In-Cabin and On-Roadway, Aerosol Sci. Tech., 45, 234–243, https://doi.org/10.1080/02786826.2010.531792, 2011.

Xu, B., Chen, X., and Xiong, J.: Air quality inside motor vehicles' cabins: A review, Indoor Built Environ., 27, 452–465, https://doi.org/10.1177/1420326X16679217, 2018.

Yin, C., Li, H., Cha, Y., Zhang, S., Du, J., Li, Z., and Ye, W.: Characterizing in-cabin air quality and vehicular air filtering performance for passenger cars in China, Environ. Pollut., 318, 120884, https://doi.org/10.1016/j.envpol.2022.120884, 2023.

Zareba, M., Weglinska, E., and Danek, T.: Air pollution seasons in urban moderate climate areas through big data analytics, Sci. Rep., 14, 3058, https://doi.org/10.1038/s41598-024-52733-w, 2024.

Zhang, C. L., Maccarone, J. R., Grady, S. T., Collins, C. M., Moy, M. L., Hart, J. E., Kang, C.-M., Coull, B. A., Schwartz, J. D., Koutrakis, P., and Garshick, E.: Indoor and ambient black carbon and fine particulate matter associations with blood biomarkers in COPD patients, Sci. Total Environ., 927, 171897, https://doi.org/10.1016/j.scitotenv.2024.171897, 2024.